Experimental verification of amplitude death induced by a periodic time-varying delay-connection

Noname manuscript No.
(will be inserted by the editor)

Experimental verification of amplitude death induced by a periodic time-varying delay-connection

Yoshiki Sugitani · Keiji Konishi · Naoyuki Hara

Received: date / Accepted: date

Abstract The present paper provides an experimental verification of amplitude death induced by a periodic time-varying delay-connection in a pair of double-scroll chaotic circuits. The connection is experimentally confirmed to enlarge the death region in a connection-parameter space, as compared with a well-known time-invariant delay-connection. The region observed in our circuit experiments agrees well with the analytical results.

Keywords amplitude death · time-varying delay · delayed feedback control · chaotic circuits

1 Introduction

Amplitude death, an interaction induced stabilization of coupled oscillators, is of considerable concern in the field of nonlinear science [1–3]. This phenomenon can occur in *non-identical* oscillators coupled by a diffusive-connection. However, it is analytically guaranteed that amplitude death never occurs in diffusively coupled *identical* oscillators [3–6]. Reddy *et al.* reported that a transmission delay in connections can induce amplitude death even in diffusively coupled *identical* oscillators [7]. This report has stimulated interest in research on amplitude death. The time-delay-induced amplitude death and other connection-induced amplitude death have been investigated analytically and experimentally for more than ten years [8–18].

If an oscillatory behavior in coupled nonlinear systems is undesirable, amplitude death is found to be a useful phenomenon for the suppression of oscillatory behavior. However, it should be noted that amplitude death is not induced by diffusive *long*-delay connections, which indicates that amplitude death cannot be used for the situation in which each nonlinear system is located far from the other systems or the situation in which nonlinear systems have high-frequency oscillations. In other words, for such situations, amplitude death cannot be used to suppress undesirable oscillations. It was

Y. Sugitani, K. Konishi, N. Hara
Department of Electrical and Information Systems, Osaka Prefecture University
1–1 Gakuen-cho, Naka-ku, Sakai Osaka 599-8531, Japan
E-mail: konishi@eis.osakafu-u.ac.jp

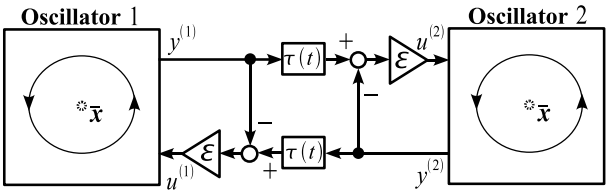

Fig. 1 Block diagram of oscillators (1) coupled by connections (2).

reported that the following two types of connections can solve this problem: distributed long-delay connections [19] and multiple long-delay connections [20]. Unfortunately, we found that it would not be easy to realize the distributed delay connections in engineering situations[1] and that the cost of multiple delay connections would be higher.

Recently, our previous report indicated that a periodic time-varying delay-connection can induce amplitude death even with a long-delay connection [21]. This connection can be easily realized and its realization would not be costly. As such, this connection is a strong candidate for death induction. The report analytically investigated the stability of amplitude death in a pair of two-dimensional prototype limit-cycle oscillators and provided a systematic procedure to design connection parameters. To the best of our knowledge, however, there has been no experimental verification of such analytical results.

The present paper provides an experimental verification of amplitude death induced by the periodic time-varying delay-connection in a pair of well-known double-scroll chaotic circuits. The chaotic circuits are implemented by popular-priced circuit devices, and the time-varying delay connections are mainly realized by peripheral interface controllers (PICs). It is experimentally confirmed that the time-varying delay-connection enlarges the death region in a connection-parameter space, as compared with the time-invariant delay-connection. Furthermore, we show that the region observed in our circuit experiments agrees well with the analytical results.

2 Oscillators coupled by time-varying connection

Our previous study considered only the two-dimensional prototype limit cycle oscillators [21]. In contrast, the present paper deals with m-dimensional nonlinear oscillators (see Fig. 1),

$$\begin{aligned} \dot{\boldsymbol{x}}^{(1,2)} &= \boldsymbol{F}\left(\boldsymbol{x}^{(1,2)}\right) + \boldsymbol{b}u^{(1,2)}, \\ y^{(1,2)} &= \boldsymbol{c}\boldsymbol{x}^{(1,2)}, \end{aligned} \tag{1}$$

where $\boldsymbol{x}^{(1,2)} \in \boldsymbol{R}^m$ are the state variables and $u^{(1,2)} \in \boldsymbol{R}$ are the connection signals. $y^{(1,2)} \in \boldsymbol{R}$ are the output signals. $\boldsymbol{b} \in \boldsymbol{R}^m$ and $\boldsymbol{c} \in \boldsymbol{R}^{1\times m}$ are the input and output vectors, respectively. There is assumed to exist at least one fixed point, $\bar{\boldsymbol{x}} : \boldsymbol{F}(\bar{\boldsymbol{x}}) = \boldsymbol{0}$, in each oscillator without coupling (i.e., $u^{(1,2)} \equiv 0$). The time-varying delay-connections are described by

$$u^{(1,2)} = \varepsilon\left\{y^{(2,1)}_{\tau(t)} - y^{(1,2)}\right\}. \tag{2}$$

[1] This is because the distributed delay connection requires an integral calculation in real time.

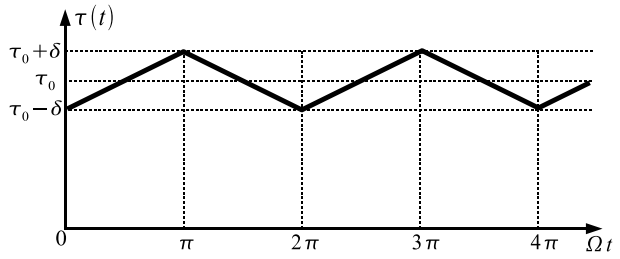

Fig. 2 Time-varying delay $\tau(t)$: periodic sawtooth type function (4).

The connection signals are proportional to the difference between the current $y^{(1,2)}$ and past $y^{(2,1)}_{\tau(t)} := y^{(2,1)}(t-\tau(t))$ output signals. The proportional constant $\varepsilon \geq 0$ denotes the coupling strength. The time delay $\tau(t) \geq 0$ is varied periodically around a nominal delay $\tau_0 > 0$ with amplitude $\delta \in [0, \tau_0]$, as illustrated in Fig. 2,

$$\tau(t) := \tau_0 + \delta f(\Omega t). \tag{3}$$

Here, $\Omega > 0$ is the frequency of variation, and $f(x)$ is the periodic sawtooth type function,

$$f(x) := \begin{cases} +\dfrac{2}{\pi}\left(x - \dfrac{\pi}{2} - 2n\pi\right) & \text{if } x \in [2n\pi, (2n+1)\pi), \\ -\dfrac{2}{\pi}\left(x - \dfrac{3\pi}{2} - 2n\pi\right) & \text{if } x \in [(2n+1)\pi, 2(n+1)\pi), \end{cases} \tag{4}$$

for $n = 0, 1, \ldots$. The reasons the present paper employs this function are as follows: it can be easily implemented in practical situations; the stability analysis is simplified by using the function.

The homogeneous steady state of oscillators (1) with connections (2) is $\left[\boldsymbol{x}^{(1)^T}\ \boldsymbol{x}^{(2)^T}\right]^T = \left[\bar{\boldsymbol{x}}^T\ \bar{\boldsymbol{x}}^T\right]^T$. Next, oscillators (1) with connections (2) are linearized around the homogeneous state,

$$\Delta\dot{\boldsymbol{x}}^{(1,2)} = \boldsymbol{A}\Delta\boldsymbol{x}^{(1,2)} + \varepsilon\boldsymbol{b}\boldsymbol{c}\left\{\Delta\boldsymbol{x}^{(2,1)}_{\tau(t)} - \Delta\boldsymbol{x}^{(1,2)}\right\}, \tag{5}$$

where $\Delta\boldsymbol{x}^{(1,2)} := \boldsymbol{x}^{(1,2)} - \bar{\boldsymbol{x}}$, $\Delta\boldsymbol{x}^{(2,1)}_{\tau(t)} := \Delta\boldsymbol{x}^{(2,1)}(t-\tau(t))$, and $\boldsymbol{A} := \{\partial\boldsymbol{F}(\boldsymbol{x})/\partial\boldsymbol{x}\}_{\boldsymbol{x}=\bar{\boldsymbol{x}}}$. Time-varying linear systems (5) can be rewritten as

$$\dot{\mathbf{x}}(t) = \mathbf{A}\mathbf{x}(t) + \mathbf{B}\mathbf{x}(t-\tau(t)), \tag{6}$$

where

$$\mathbf{x}(t) := \begin{bmatrix}\Delta\boldsymbol{x}^{(1)} \\ \Delta\boldsymbol{x}^{(2)}\end{bmatrix},\ \mathbf{A} := \begin{bmatrix}\boldsymbol{A} - \varepsilon\boldsymbol{b}\boldsymbol{c} & \boldsymbol{0} \\ \boldsymbol{0} & \boldsymbol{A} - \varepsilon\boldsymbol{b}\boldsymbol{c}\end{bmatrix},\ \mathbf{B} := \begin{bmatrix}\boldsymbol{0} & \varepsilon\boldsymbol{b}\boldsymbol{c} \\ \varepsilon\boldsymbol{b}\boldsymbol{c} & \boldsymbol{0}\end{bmatrix}.$$

From [22], it is obvious that if a time-invariant comparison system,

$$\dot{\mathbf{x}}(t) = \mathbf{A}\mathbf{x}(t) + \frac{1}{2\delta}\mathbf{B}\int_{t-\tau_0-\delta}^{t-\tau_0+\delta}\mathbf{x}(s)\mathrm{d}s, \tag{7}$$

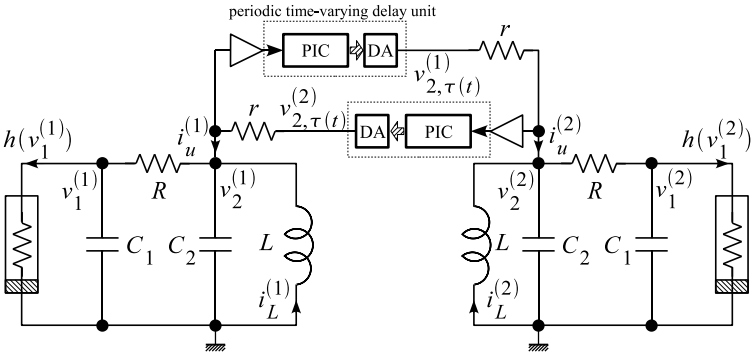

Fig. 3 Circuit diagrams of double-scroll chaotic circuits coupled by time-varying connections.

is asymptotically stable, then time-varying linear system (6) with sufficiently large $\Omega \gg 0$ is stable. According to [22], the characteristic equation of system (7) is given by

$$g(\lambda) := \det\left[\lambda \boldsymbol{I} - \mathbf{A} - \mathbf{B}e^{-\lambda\tau_0} H(\lambda\delta)\right] = 0, \tag{8}$$

where

$$H(x) := \begin{cases} (\sinh x)/x & \text{if } x \neq 0 \\ 1 & \text{if } x = 0 \end{cases},$$

is often called the sinc function [23]. Here, it is easy to confirm from Eq. (8) that the odd number property holds. Namely, time-varying delay-connection (2) never stabilizes the steady state for any $\varepsilon \geq 0$ and $\tau(t) \geq 0$ if $\boldsymbol{A}$ has an odd number of real positive eigenvalues.

3 Coupled double-scroll chaotic circuits

3.1 Circuit equations

Let us consider two double-scroll chaotic circuits [24] illustrated in Fig. 3,

$$\begin{cases} C_1 \dfrac{\mathrm{d}v_1^{(1,2)}}{\mathrm{d}t} = \dfrac{1}{R}\left(v_2^{(1,2)} - v_1^{(1,2)}\right) - h\left(v_1^{(1,2)}\right) \\ C_2 \dfrac{\mathrm{d}v_2^{(1,2)}}{\mathrm{d}t} = \dfrac{1}{R}\left(v_1^{(1,2)} - v_2^{(1,2)}\right) + i_{\mathrm{L}}^{(1,2)} + i_u^{(1,2)} \\ L \dfrac{\mathrm{d}i_{\mathrm{L}}^{(1,2)}}{\mathrm{d}t} = -v_2^{(1,2)} \end{cases}. \tag{9}$$

Here, $v_1^{(1,2)}$ [V], $v_2^{(1,2)}$ [V], and $i_{\mathrm{L}}^{(1,2)}$ [A] are the voltages across C_1 [F], C_2 [F], and the current through L [H], respectively. The currents through the nonlinear resistors, $h\left(v_1^{(1,2)}\right)$ [A], are given by

$$h(v) := m_0 v + \frac{1}{2}(m_1 - m_0)\left|v + B_{\mathrm{p}}\right| + \frac{1}{2}(m_0 - m_1)\left|v - B_{\mathrm{p}}\right|.$$

The currents through the connection resistors r,

$$i_u^{(1,2)} = \frac{1}{r}\left(v_{2,\tau(t)}^{(2,1)} - v_2^{(1,2)}\right), \tag{10}$$

flow into C_2, where $v_{2,\tau(t)}^{(2,1)} := v_2^{(2,1)}(t-\tau(t))$ are the delayed voltages.

Double-scroll circuits (9) can be transformed into dimensionless form (1) with

$$\boldsymbol{F}(\boldsymbol{x}) := \begin{bmatrix} \eta\left\{x_2 - x_1 - g(x_1)\right\} \\ x_1 - x_2 + x_3 \\ -\gamma x_2 \end{bmatrix},\ \boldsymbol{b} = \begin{bmatrix} 0 \\ 1 \\ 0 \end{bmatrix},\ \boldsymbol{c} = \begin{bmatrix} 0 \\ 1 \\ 0 \end{bmatrix}^T, \tag{11}$$

where

$$\begin{aligned} &x_1 := \frac{v_1}{B_\mathrm{p}},\ x_2 := \frac{v_2}{B_\mathrm{p}},\ x_3 := \frac{i_L R}{B_\mathrm{p}},\ \eta := \frac{C_2}{C_1},\ \gamma := \frac{R^2 C_2}{L}, \\ &a := m_1 R,\ b := m_0 R, \\ &g(x) := bx + \frac{1}{2}(b-a)\left\{|x-1| - |x+1|\right\}. \end{aligned}$$

Note that the dimensionless time $t/(RC_2)$ is used in form (1) instead of the real time t. Each isolated oscillator (i.e., $u^{(1,2)} \equiv 0$) has three fixed points: $\bar{\boldsymbol{x}}_\pm := \left[\pm p\ 0\ \mp p\right]^T$ and $\bar{\boldsymbol{x}}_0 := \boldsymbol{0}$, where $p := (b-a)/(b+1)$.

3.2 Stability analysis

In order to simplify the discussion below, the present paper focuses on the stabilization of $\bar{\boldsymbol{x}}_+$ [2]. The dynamics of oscillators (1) coupled by connections (2) around $\bar{\boldsymbol{x}}_+$ is described by Eq. (6), where

$$\boldsymbol{A} = \begin{bmatrix} -\eta(b+1) & \eta & 0 \\ 1 & -1 & 1 \\ 0 & -\gamma & 0 \end{bmatrix},\ \varepsilon = \frac{R}{r}.$$

Equation (8) can be described by $g(\lambda) = g_1(\lambda)g_2(\lambda)$, where the quasi-polynomial functions $g_{1,2}(\lambda)$ are denoted by

$$\begin{aligned} g_1(\lambda) &:= (\lambda + \bar{\eta})\left\{\lambda^2 + \lambda + \gamma + \varepsilon\lambda\left(1 + H(\lambda\delta)\, e^{-\lambda\tau_0}\right)\right\} - \lambda\eta, \\ g_2(\lambda) &:= (\lambda + \bar{\eta})\left\{\lambda^2 + \lambda + \gamma + \varepsilon\lambda\left(1 - H(\lambda\delta)\, e^{-\lambda\tau_0}\right)\right\} - \lambda\eta, \end{aligned} \tag{12}$$

and $\bar{\eta} := \eta(1+b)$. The homogeneous steady state $\left[\bar{\boldsymbol{x}}_+^T\ \bar{\boldsymbol{x}}_+^T\right]^T$ is stable if and only if all of the roots λ for both $g_1(\lambda) = 0$ and $g_2(\lambda) = 0$ have negative real parts. Next, let us consider the stability of $g_1(\lambda) = 0$. The real and imaginary parts of $g_1(i\lambda_I) = 0$, $\lambda_I \in \boldsymbol{R}$, are given by

$$\begin{aligned} &\bar{\eta}\lambda_I\Phi(\lambda_I)\varepsilon\sin\lambda_I\tau_0 - \lambda_I^2\Phi(\lambda_I)\varepsilon\cos\lambda_I\tau_0 + \theta_R(\lambda_I) - \lambda_I^2\varepsilon = 0, \\ &\lambda_I^2\Phi(\lambda_I)\varepsilon\sin\lambda_I\tau_0 + \bar{\eta}\lambda_I\Phi(\lambda_I)\varepsilon\cos\lambda_I\tau_0 + \theta_I(\lambda_I) + \bar{\eta}\lambda_I\varepsilon = 0, \end{aligned} \tag{13}$$

[2] The same results are obtained for $\bar{\boldsymbol{x}}_-$. Since matrix $\boldsymbol{A}$ around $\bar{\boldsymbol{x}}_0$ satisfies the odd number property, we do not have to consider the stabilization of $\bar{\boldsymbol{x}}_0$.

where $\theta_R(\lambda_I) := -\lambda_I^2(\bar{\eta}+1) + \bar{\eta}\gamma$, $\theta_I(\lambda_I) := \lambda_I\left(\gamma + \eta b - \lambda_I^2\right)$, and

$$\Phi(\lambda_I) := \begin{cases} (\sin\lambda_I\delta)/(\lambda_I\delta) & \text{if } \lambda_I\delta \neq 0, \\ 1 & \text{if } \lambda_I\delta = 0. \end{cases} \tag{14}$$

Equation (13) can be transformed into

$$F(\varepsilon,\lambda_I) := \lambda_I^2\left(\bar{\eta}^2+\lambda_I^2\right)\left\{1-\Phi(\lambda_I)^2\right\}\varepsilon^2 + 2\lambda_I\left\{\bar{\eta}\theta_I(\lambda_I) - \lambda_I\theta_R(\lambda_I)\right\}\varepsilon + \theta_R(\lambda_I)^2 + \theta_I(\lambda_I)^2 = 0, \tag{15}$$

which describes the relation between ε and λ_I and does not depend on τ_0. Using Eq. (15), the boundary curves of $g_1(\lambda) = 0$ are obtained by the procedure proposed in our previous paper [21]. The boundary curves of $g_2(\lambda) = 0$ are also obtained by the same procedure.

The parameters of dimensionless form (11) are fixed at

$$\eta = 10,\ \gamma = 18,\ a = -1.36,\ b = -0.74. \tag{16}$$

The curves and the regions for the time-invariant delay-connection (i.e., $\delta = 0$) are illustrated in Fig. 4(a). The solutions of $g_1(i\lambda_I) = 0$ and $g_2(i\lambda_I) = 0$ are described by the black and red curves, respectively. The thin (bold) curves indicate that a root of $g_{1,2}(i\lambda_I) = 0$ crosses the imaginary axis from left to right (right to left). There exist two narrow stability regions (i.e., shaded regions) for $0.3 \lesssim \tau_0 \lesssim 1.5$. Note that the long-delay connection (i.e., $\tau_0 \gtrsim 2$) never induces death for any ε. In contrast, for the time-varying delay-connection with $\delta = 0.75$, as shown in Fig. 4(b), there exists no curve in the wide range $\varepsilon > 0.528$ on the ε–τ_0 plane. This result analytically implies that there is no upper limit of τ_0 in the range. The unstable steady state can be stabilized by the arbitrarily long nominal delay τ_0 when ε is set within the range.

4 Circuit experiments

The two double-scroll chaotic circuits illustrated in Fig. 3 are implemented by popular-priced circuit devices (see Fig. 5(a)). The nonlinear resistors have the same structure as in [25]. The inductors are realized by general impedance converters consisting of four resistors, one capacitor, and two operational amplifiers [26]. The periodic time-varying delay units (broken-line rectangles in Fig. 3) are implemented by PIC (PIC18F2550) devices and digital-to-analog converters (DAs). The voltages $v_2^{(1,2)}$ are applied to the PIC devices via the voltage buffers and are imported through their built-in analog-digital converters. The imported data are processed by the software program such that the digitalized signals corresponding to the delayed voltages are exported. The digitalized signals are transformed into the delayed analog voltages $v_{2,\tau(t)}^{(1,2)} := v_2^{(1,2)}(t-\tau(t))$ by the DAs using the R/2R resistor network. The detailed circuit structure and its operation are explained in Appendix A.

The parameters of dimensionless form (11), i.e., Eq. (16), are equivalent to the circuit parameters,

$$C_1 = 0.1\times10^{-6}\ \text{F},\ C_2 = 1.0\times10^{-6}\ \text{F},\ L = 180\times10^{-3}\ \text{H},\ R = 1,800\ \Omega,$$
$$B_p = 1.0\ \text{V},\ m_0 = -0.4\times10^{-3},\ m_1 = -0.8\times10^{-3},$$

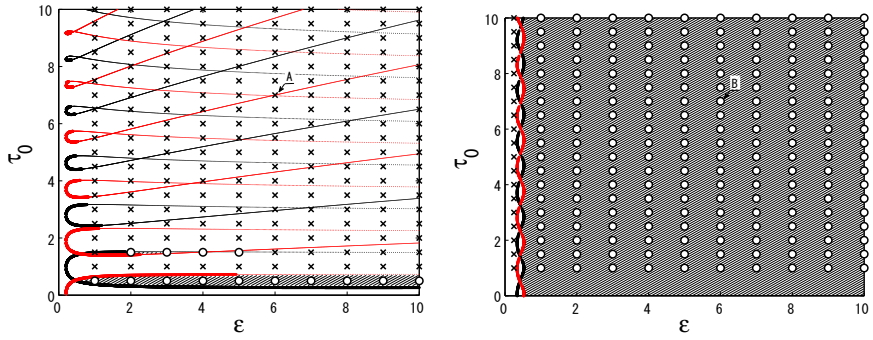

(a) (b)

Fig. 4 Stability regions in the ε–τ_0 plane: (a) time-invariant delay-connection ($\delta = 0$), (b) time-varying delay-connection ($\delta = 0.75, \Omega = 19$). The curves and shaded areas are the stability boundaries and the stability regions, which are analytically estimated by Eq. (15). The black and red curves are the solutions of $g_1(i\lambda_I) = 0$ and $g_2(i\lambda_I) = 0$, respectively. The symbols ◯ (×) denote the occurrence (non-occurrence) of stabilization experimentally.

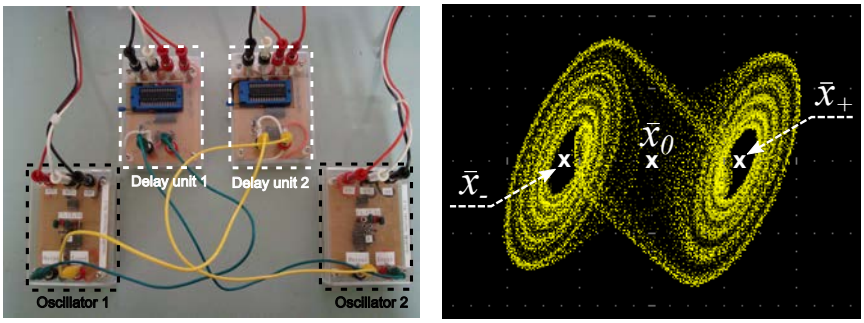

(a) (b)

Fig. 5 Photograph of the actual circuits and double-scroll chaotic attractor: (a) photograph of the actual circuits illustrated in Fig. 3, (b) double-scroll chaotic attractor in each circuit (Horizontal axis: v_1 (2 V/div); vertical axis: v_2 (500 mV/div)).

where a double-scroll chaotic attractor exists in each isolated oscillator, as shown in Fig. 5(b). Three unstable fixed points, $\bar{\boldsymbol{x}}_\pm$ and $\bar{\boldsymbol{x}}_0$, coexist with the attractor. We have experimentally checked whether amplitude death occurs for various connection parameters. The frequency of periodic time delay $\tau(t)$ denoted by Eq. (3) is fixed at a large value $\Omega = 19$. The symbols ◯ (×) in Fig. 4 denote the parameter set (ε, τ_0) where the stabilization (non-stabilization) is experimentally observed. The stability region on the analytical estimation (i.e., shaded regions) roughly agrees with the circuit experiments (i.e., set of ◯). Let us, as an example, focus on the parameter set $(\varepsilon = 6, \tau_0 = 7)$ illustrated by points A and B in Fig. 4. The time series data of the

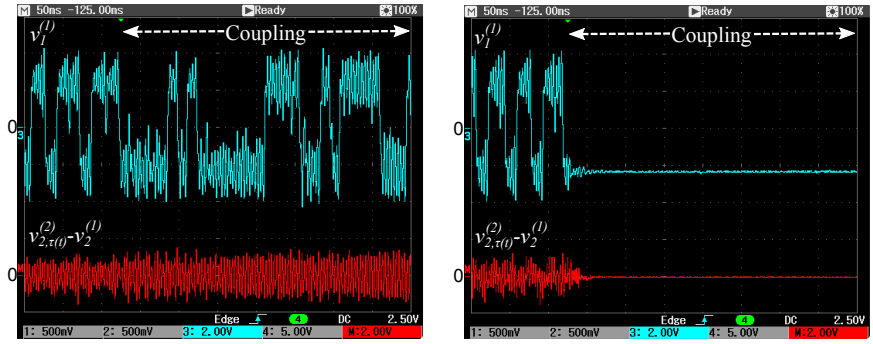

(a) (b)

Fig. 6 Time series data of $v_1^{(1)}$ and $v_{2,\tau(t)}^{(2)} - v_2^{(1)}$ for parameter set ($\varepsilon = 6$, $\tau_0 = 7$): (a) point A ($\delta = 0$) and (b) point B ($\delta = 0.75$ and $\Omega = 19$) in Fig. 4. Horizontal axis: 50 ms/div; vertical axis: 2 V/div.

voltage $v_1^{(1)}$ and the potential difference $v_{2,\tau(t)}^{(2)} - v_2^{(1)}$, which is proportional to the connection current (10), with the time-invariant connection ($\delta = 0$) and the time-varying connection ($\delta = 0.75$) are illustrated in Figs. 6(a) and 6(b), respectively. The two circuits are connected at time $t = 125$ ms. For the time-invariant connection, $v_1^{(1)}$ and $v_{2,\tau(t)}^{(2)} - v_2^{(1)}$ do not converge on the steady state and the zero, respectively, due to long-delay connections. For the time-varying connection, they converge on the steady state and the zero, respectively, even with long-delay connections. Our experimental results suggest that the analytical results reported in our previous study [21] are valid for real systems. Therefore, we conclude that the time-varying delay-connection is a useful and practical scheme for death induction.

5 Discussion

The preceding section demonstrated that the analytical results agree with the experimental results under which the frequency of variations, Ω, is sufficiently large. However, it is obvious that the sufficiently large Ω is not easy to implement in real systems. From a practical point of view, it is desirable to know its lower limit frequency Ω, with which the analytical results agree with the experimental results. Since it is difficult to derive such Ω analytically, this section experimentally examines the dependence on Ω.

Figures 7(a) and 7(b) show the stability regions in the ε–τ_0 plane for $\Omega = 0.21$ and $\Omega = 0.52$, respectively. The other parameters are the same as in Fig. 4(b). Figures 4(b) and 7 show that the experimental results do not agree with the analytical results for small Ω. It can be seen that the stability region for small Ω has a similar shape to that for the time-invariant delay-connection. In order to examine the dependence on Ω, we define a matching ratio, $\beta := N_\mathrm{e}/N_\mathrm{a}$, where N_a is the number of stable points within the analytical stability region on $\varepsilon \in [0, 10]$ and $\tau_0 \in [\delta, 10]$. The number of points at which the stabilization occurs in the circuit experiments is denoted by N_e. Here,

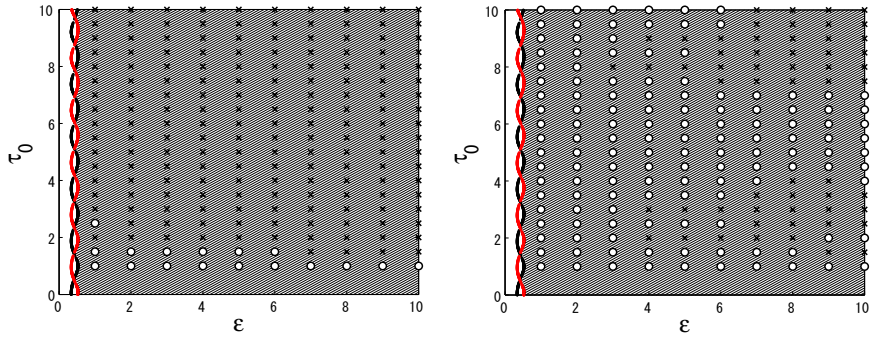

(a) (b)

Fig. 7 Stability regions in the ε–τ_0 plane for $\delta = 0.75$: curves, shaded area, and symbols ◯ ($\times$) are the same as in Fig. 4; (a) $\Omega = 0.21$ ($\beta = 0.08947$) and (b) $\Omega = 0.52$ ($\beta = 0.7$).

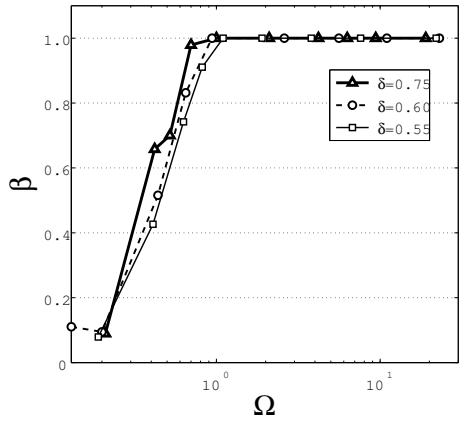

Fig. 8 Matching ratio β versus frequency Ω for $\delta = 0.75$, 0.60, and 0.55. The parameters are the same as in Figs. 4(b) and 7.

$\beta \simeq 1$ indicates that the experimental region approximately agrees with the analytical region, as shown in Fig. 4(b). In contrast, $\beta \simeq 0$ implies that the experimental region does not agree with the analytical region at all, as shown in Fig. 7(a). The relations between β and Ω for $\delta = 0.75$, 0.60, and 0.55 are illustrated in Fig. 8. It can be seen that β increases with Ω, and then reaches $\beta \simeq 1$ at $\Omega \simeq 1$. This fact does not depend greatly on δ. Figure 8 suggests that the experimental region approximately agrees with the analytical region for $\Omega \gtrsim 1$.

From another practical point of view, we have to consider the existence of mismatch in frequencies Ω between the two delay units, since it is difficult to realize the identical units in real systems. Our numerical simulations suggested that a slight mismatch does not shrink the stability regions; however, the behavior with a significant mismatch has not been investigated. This would be an important future work.

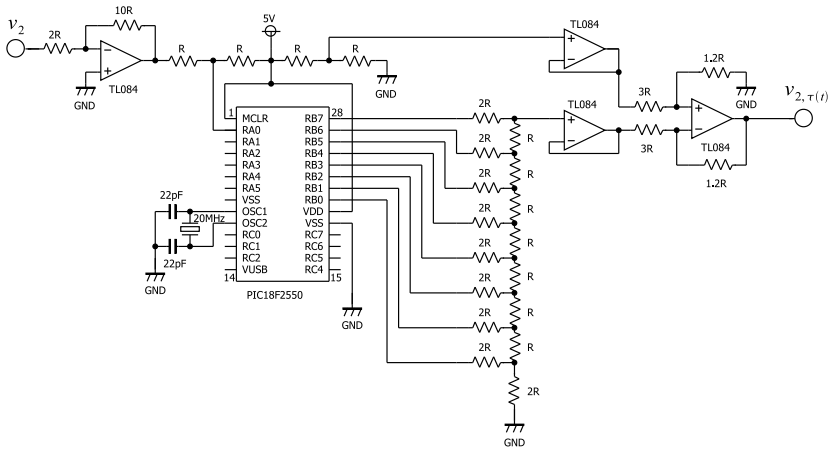

Fig. 9 Sketch of the circuit diagram of the periodic time-varying delay unit ($R = 1,000\ \Omega$).

6 Conclusion

Amplitude death induced by a periodic time-varying delay-connection is experimentally observed in a pair of the double-scroll chaotic circuits. It is experimentally confirmed that the connection enlarges the death region in the connection-parameter space, as compared with the time-invariant delay-connection. The region observed in our circuit experiments agrees well with the analytical results.

Acknowledgments

The present research was partially supported by JSPS KAKENHI (23560538).

A Implementation of the time-varying delay unit

A circuit diagram of the periodic time-varying delay unit represented by the dotted-line rectangle in Fig. 3 is presented in Fig. 9. Since PIC (PIC18F2550) can deal with the input voltages only within a voltage range ($0 - 5$ V), v_2 is shifted to the range at a stage prior to PIC. The shifted v_2 is applied to an input terminal RA0 and is fed into PIC through its built-in analog-digital converter. PIC processes the sampled v_2 into periodic time-varying delayed $v_{2,\tau(t)}$. This process is explained below. The eight bits $v_{2,\tau(t)}$ are exported from output terminals RB0 to RB7 to the digital-analog (DA) converter using the R/2R resistor network. The output of the DA converter is shifted back to the original voltage range.

In order to check the input-output relation of this unit, as shown in Fig. 10(a), the sinusoidal wave voltage represented by the solid yellow curve is applied to the unit. The output voltage with $\delta = 0$ (solid red curve) which corresponds to the time-invariant delay-connection and that with $\delta = 0.25$ and $\Omega = 13$ (solid blue curve) are observed. It can be seen that the voltage with $\delta = 0.25$ consists of the time-invariant delayed voltage and the high-frequency oscillation. These results indicate that the periodic time-varying delay unit works properly. Next, we explain the algorithm that processes the sampled v_2 into $v_{2,\tau(t)}$. This algorithm is realized by the first-in, first-out (FIFO) queue (see Fig. 10(b)). The sampled v_2 is periodically stored from the left into the buffers on the FIFO queue. The stored data is sequentially shifted to the right-hand neighbor buffer in the manner of a bucket brigade. The algorithm selects

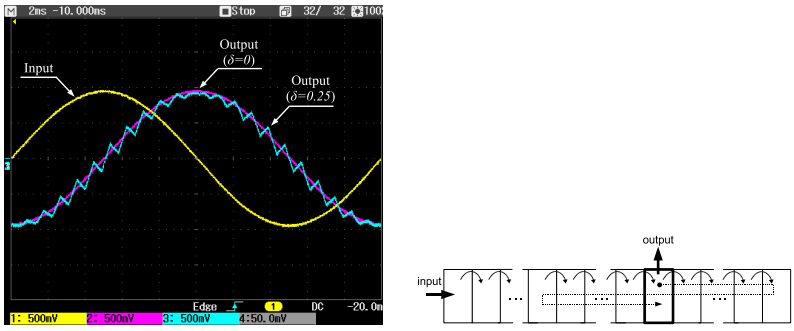

(a) (b)

Fig. 10 Input and output voltages of the periodic time-varying connection unit and sketch of the FIFO queue in PIC: (a) input and output voltages (Horizontal axis: 2 ms/div; vertical axis: 500 mV/div) and (b) shifted data on the FIFO queue with 218 buffers.

data from the buffer represented by the bold-line rectangle, and then outputs the data. The delay time is estimated by the product of the number of buffers between the extreme left buffer and the output buffer and the shifting period (25 μs). The output buffer is periodically moved on the FIFO queue, and the delay time of the output data is then periodically varied.

References

1. Pikovsky, A., Rosenblum, M., and Kurths, J.: *Synchronization*. Cambridge University Press (2001).
2. Yamaguchi, Y. and Shimizu, H.: Theory of self-synchronization in the presence of native frequency distribution and external noises. *Physica D* **11**, 212–226 (1984).
3. Aronson D.G., Ermentrout, G.B., and Kopell, N.: Amplitude response of coupled oscillators. *Physica D* **41**, 403–449 (1990).
4. Konishi, K.: Limitation of time-delay induced amplitude death. *Phys. Lett. A* **341**, 401–409 (2005).
5. Michiels, W. and Nijmeijer, H.: Synchronization of delay-coupled nonlinear oscillators: An approach based on the stability analysis of synchronized equilibria. *Chaos* **19**, 033110 (2009).
6. Konishi, K. and Hara, N.: Topology-free stability of a steady state in network systems with dynamic connections. *Phys. Rev. E* **83**, 036204 (2011).
7. Reddy, D.V.R., Sen, A., and Johnston, G.L.: Time delay induced death in coupled limit cycle oscillators. *Phys. Rev. Lett.* **80**, 5109–5112 (1998).
8. Strogatz, S.H.: Death by delay. *Nature* **394**, 316–317 (1998).
9. Reddy, D.V.R., Sen, A., and Johnston, G.L.: Experimental evidence of time-delay-induced death in coupled limit-cycle oscillators. *Phys. Rev. Lett.* **85**, 3381–3384 (2000).
10. Herrero, R., Figueras, M., Rius, J., Pi, F., and Orriols, G.: Experimental observation of the amplitude death effect in two coupled nonlinear oscillators. *Phys. Rev. Lett.* **84**, 5312–5315 (2000).
11. Konishi, K.: Time-delay-induced stabilization of coupled discrete-time systems. *Phys. Rev. E* **67**, 017201 (2003).
12. Mehta, M.P. and Sen, A.: Death island boundaries for delay-coupled oscillator chains. *Phys. Lett. A* **355**, 202–206 (2006).
13. Atay, F.M.: Oscillator death in coupled functional differential equations near Hopf bifurcation. *J. Diff. Eqns.* **221**, 190–209 (2006).

14. Karnatak, R., Ramaswamy, R., and Prasad, A.: Amplitude death in the absence of time delays in identical coupled oscillators. *Phys. Rev. E* **76**, 035201 (2007).
15. Karnatak, R., Ramaswamy, R., and Prasad, A.: Synchronization regimes in conjugate coupled chaotic oscillators. *Chaos* **19**, 033143 (2009).
16. Singla, T., Pawar, N., and Parmananda, P.: Exploring the dynamics of conjugate coupled Chua circuits: simulations and experiments. *Phys. Rev. E* **83**, 026210 (2011).
17. Zhang, X., Wu, Y., and Peng, J.: Analytical conditions for amplitude death induced by conjugate variable couplings. *Int. J. of Bifurcations and Chaos* **21**, 225–235 (2011).
18. Konishi, K., Senda, K., and Kokame, H.: Amplitude death in time-delay nonlinear oscillators coupled by diffusive connections. *Phys. Rev. E* **78**, 056216 (2008).
19. Atay, F.M.: Distributed delays facilitate amplitude death of coupled oscillators. *Phys. Rev. Lett.* **91**, 094101 (2003).
20. Konishi, K., Kokame, H., and Hara, N.: Stabilization of a steady state in network oscillators by using diffusive connections with two long time delays. *Phys. Rev. E* **81**, 016201 (2010).
21. Konishi, K., Kokame, H., and Hara, N.: Stability analysis and design of amplitude death induced by a time-varying delay connection. *Phys. Lett. A* **374**, 733–738 (2010).
22. Michiels, W., Assche, V.V., and Niculescu, S.-I.: Stabilization of time-delay systems with a controlled time-varying delay and applications. *IEEE Trans. Automatic Control* **50**, 493–504 (2005).
23. Gearhart, W.B. and Shultz, H.S.: The function sinx/x. *College Math. J.* **21**, 90–99 (1990).
24. Matsumoto, T., Chua, L.O., and Komuro, M.: The double scroll. *IEEE Trans. Circuits and Sys.* **32**, 797–818 (1985).
25. Kennedy, M.P.: Robust op amp realization of Chua's circuit. *Frequenz* **46**, 66–80 (1992).
26. Itoh, M.: Synthesis of electronic circuits for simulating nonlinear dynamics. *Int. J. of Bifurcations and Chaos* **11**, 605–653 (2001).